

Chapter 2

Physical and Mechanical Properties of Surface Nanocrystalline Structures Generated by Severe Thermal-Plastic Deformation

Hryhoriy Nykyforchyn, Volodymyr Kyryliv and Olga Maksymiv

2.1 Introduction

Improvement of mechanical properties of engineering steels due to the formation of nanocrystalline structures (NCS) is generally done by severe plastic deformation. Both volume and surface NCS can be achieved by this type of treatment [8, 13, 14, 23, 25, 26]. One method for the creation of surface NCS consists in severe thermal-plastic deformation by high-speed friction. A technology for the formation of surface gradient NCS is developed on this base by mechanical-pulse treatment (MPT) [11, 17] which is based on the principles of grinding process (Fig. 2.1). A special metal tool is installed instead of a grinding ring.

A lathe equipped by the special device similar to spindle mandrel of a grinder can be used for the treatment of cylindrical surfaces. This tool rotates with velocity V_1 of 50–70 m/s and the treated component rotates at $V_2 = 0.03$ –0.18 m/s. The tool pressure on treated component surface in the friction contact zone reaches 1 GPa at a depth of run of $t = 0.25$ –0.35 mm and the longitudinal feed of $S = 0.3$ –4 mm/rev. The coolant is brought up into the friction area. Its role consists not only in rapid cooling of thermal-plastic-deformed surface layer but also in its alloying. The surface temperature in the friction contact area depends on the treatment regimes and varies between 1100 and 1600 K.

The applied coolants are oil or water based with different polymer additives. The thermal and mechanical destruction of the additives in the contact area under high pressure and temperature create active carbon, hydrogen, oxygen and other alloying elements [10, 12]. The rapid plastic deformation and high temperature promote a mass transfer at abnormally high diffusion velocity of $D = 10^{-6}$ – 10^{-7} m²/s [12]. In particular, a special oil-base coolant with low molecular weight polyethylene

H. Nykyforchyn (✉) · V. Kyryliv · O. Maksymiv
Karpenko Physico-Mechanical Institute of NASU, 5 Naukova Str.,
79060 Lviv, Ukraine

H. Nykyforchyn
+38 (032) 2632133
e-mail: nykyfor@ipm.lviv.ua

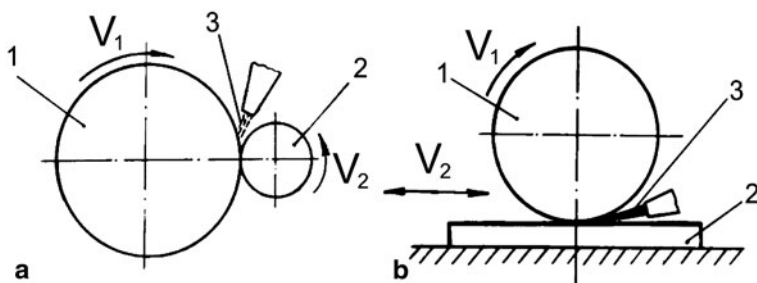


Fig. 2.1 The scheme of MPT of **a** cylindrical and **b** plane surfaces: 1—strengthening tool; 2—treated component; 3—coolant

additives was developed for saturation of surface layers with carbon [10]. This is especially useful for the treatment of low carbon steels.

The contact zone is the area with high shear deformation. Phase transformations occur in the surface layers due to high-speed heating above the phase transformation temperature and the subsequent cooling by heat sink in the coolant, the tool and the component.

The achieved nanostructure of the surface layer with a different phase composition and a modified chemical composition has different physical and mechanical properties, which are discussed in this chapter.

2.2 Investigation Methods

Armco iron and carbon steels 45 (0.45C), 40Kh (0.40 C-1Cr) and 65G (0.65 C-1Mn) with a ferrite-pearlite structure in as-received state (after annealing) were investigated. Three coolant types were used for MPT: mineral oil U-12 A (GOST 20799-88 standard), 10 % aqueous solution of emulsol and a special coolant for carbonization [11]. MPT was carried out on specimens of two geometries: (a) cylindrical specimens strengthened by a lathe and (b) flat specimens, which were strengthened by a flat grinding machine.

The cylindrical specimens were of two sizes:

- a. Specimens with net diameter of 20 mm and a length of 100 mm were used for chemical and phase analysis as well as microhardness measurements.
- b. Ring specimens with a diameter of 40 mm were used for ring-insert wear-resistance tests [11].

The counter body was a specimen of the high carbon martensite ball-bearing steel ShKh15 (1.0 C-1.5Cr). The GOST TAP-30 oil with an addition of 0.1 wt% of fine quartz sand with grain size up to 40 μm was used. The tests were performed at the loading of 4.0 MPa and the sliding velocity of 0.9 m/s. The specimens were preloaded at 0.8 MPa within 2 h.

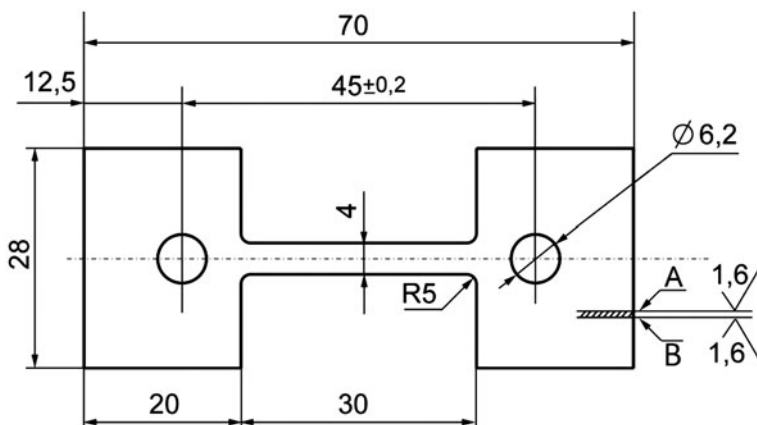


Fig. 2.2 Specimen for an evaluation of mechanical properties of tension

Two sizes of flat specimens were used as well. The tensile properties were determined using 1.6-mm thick specimens (Fig. 2.2). However, the hardening effect of the surface treatment is localized in the surface layer. To decrease the hardness gradient in the specimen cross section, they were preliminary quenched and tempered at 500°C, grinded, treated by MPT and tempered again at the same temperature. Fatigue crack growth was determined on $6 \times 19 \times 150$ -mm single-notched beam specimens under the cycle bending load with the frequency of 26 Hz and the load ratio $R = 0$.

The phase analyses were carried out metallographically and with the transmission electron microscope JEM-CX. The diffractometry analyses were performed with the diffractometer DRON-3 to measure the average grain size and the dislocation density. The dislocation density was calculated on the basis of widening of the lines $(220)_{k\alpha}$. Phase analyses of the surface layers were carried out with the $\text{CuK}\alpha$ radiation method ($U = 30$ kV, $I = 20$ mA) with a step of 0.05 and the exposition of 4 s. The diffractograms were post processed using the software Powder Cell [5]. The X-ray pictures were analysed after the Joint Committee on Powder Diffraction Standards/American Society for Testing and Materials (JCPDS-ASTM) index [19].

The carbon content in surface layers of the strengthened Armco iron was determined layer by layer by the chemical analysis. For this purpose, three layers 0.05 mm thick were cut off the specimen.

2.3 Results of Investigations and Discussion

The metallographic examination showed the presence of unetched surface area (Fig. 2.3a) with a high dislocation density, which is maximal on the surface (Fig. 2.3b, curve 1). Two types of deformation occur during friction: pressure and shear, both

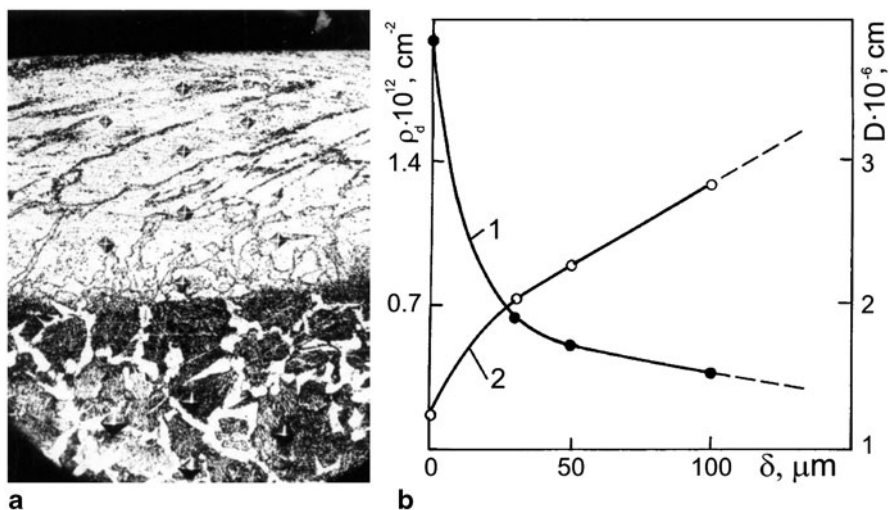


Fig. 2.3 Steel 45 after MPT ($V_2 = 1.0$ m/min; $S = 0.5$ mm/double motion; $t = 0.3$ mm) in mineral oil. **a** Microstructure ($\times 300$). **b** Dislocation density (1) and grain size (2) in a depth of strengthened layer δ

of which decrease with increasing depth δ . Shear deformation causes a particular texture, which can be distinguished by the inclination of grain groups (Fig. 2.3a).

With increasing depth from the surface, the deformation grade decreases and thus the grain size decreases (Fig. 2.3b, curve 2). The calculated average grain size d on the surface is 12 nm, which is in good agreement with the literature data [24]. The obtained data of d and ρ are comparable with those for powder iron milled in a ball mill [20]. Therefore, it can be argued that MPT and the ball milling decrease the grain size to nearly the same extent.

The phase composition changes were caused by rapid heat treatment during MPT with material temperature rising above the phase transformation point and subsequently dropping below this point. The resulting martensite–austenite microstructure includes rest of cementite that have not fully transformed during the deformation process (Fig. 2.4). The phase composition and parameters of the nanocrystalline-hardened surface layer depend on the coolant type, process parameters and the chemical compositions of the material [6].

The electron microscopy images of the microstructure of the hardened surface layer are presented in Fig. 2.5. The grain size on the surface of 10–15 nm is achieved and it grows gradually with the distance from the surface.

The grains look strongly distorted. The probable reason for it is the far field stresses in non-equilibrium grain boundaries due to high dislocation density. A cellular structure with low degrees of lattice disorientation of grains is typical at the distance from the surface of 200 μm and above. Randomly distributed dislocation clews are observed in the grains. The microstructure is strongly fragmented in the surface layer at a depth of 5 μm . Arrays of parallel nanocrystals 10–15 nm are observed in dark-field images, which is in good agreement with the diffractometry

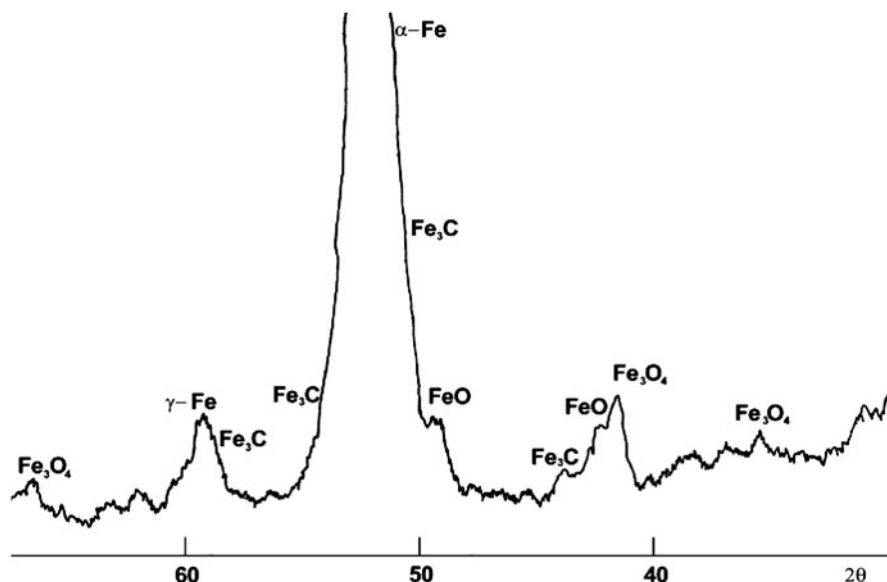


Fig. 2.4 The fragment of diffractogram of the surface layer on 45 steel after MPT in a mineral oil

(X-ray) examinations. The observed washed out rings on diffractograms are indications of a quasi-amorphous structure. The absence of the typical amorphous halo ([3]; Fig. 2.4) can be explained by deep penetration of X-rays (over $10\ \mu\text{m}$). The observed circular distribution of grains signifies big disorientation (over 10) between adjacent grains, and the azimuthal blurring is particular for large strains. With the depth increasing to $20\text{--}30\ \mu\text{m}$, the grain boundary stresses gradually decrease, the grain size increases and diffraction picture corresponds to a fine-grain microstructure. The deformation velocity $\dot{\epsilon} = 2 \times 10^3\ \text{s}^{-1}$ was calculated by using the dislocation density $\rho \approx 10^9$ (Fig. 2.3b) and the Jonston–Hilman law [4]. This means that the deformation velocity $10^3\ \text{s}^{-1}$ is required for the nanocrystalline structure formation in surface layers.

For the Armco iron, the effectiveness of carbon enrichment of surface layers by MPT with a special coolant is shown (Fig. 2.6). Carbon concentration C on the surface can reach 1 % and depend on not only the treatment process parameters [9, 12] but also the surface roughness; for polished surfaces, higher carbon enrichment can be obtained. According to Fisher [2], a linear decrease of carbon content $\lg C$ versus δ^2 occurs for volumetric diffusion and linear decrease of $\lg C$ versus δ is typical for grain-boundary diffusion. The analysis of concentration curves after MPT showed that carbon is distributed mainly on grain boundaries (Fig. 2.7).

The percentage of coolant additives in the chemical composition of the surface layers is presented in Table 2.1. The most differences were obtained for carbon and oxygen. It is known [16] that the presence of carbon at grain boundaries increases material strength, while the presence of oxygen, nitrogen and hydrogen deteriorates

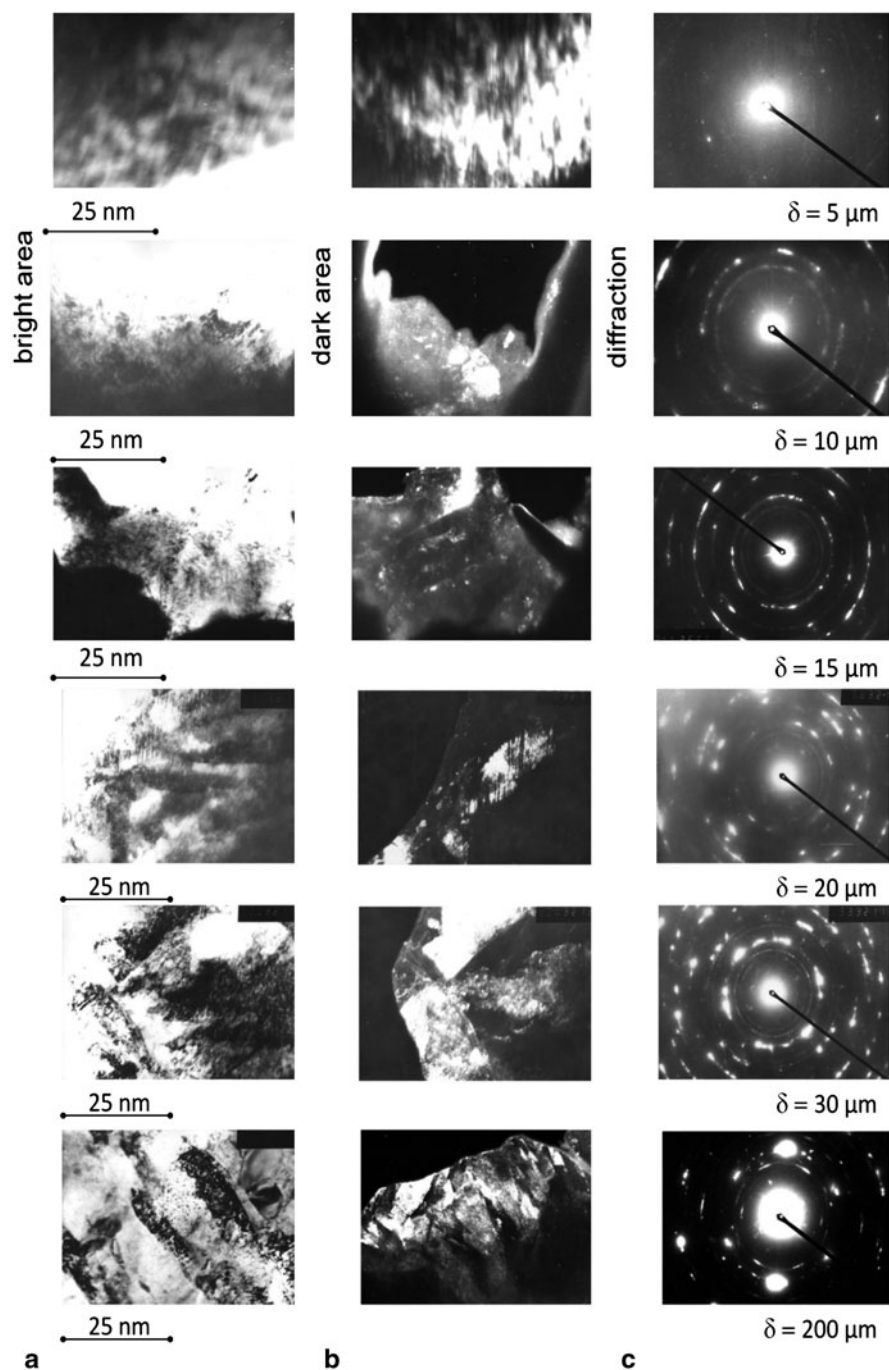


Fig. 2.5 Electron-microscope images: **a** light field, **b** dark field and **c** electronograms of nanocrystalline structures of 45 steel surface layers from the different depth δ after MPT

Fig. 2.6 Distribution of carbon in Armco iron during MPT using the special coolant for carbonization: 1—polishing, 2—grinding

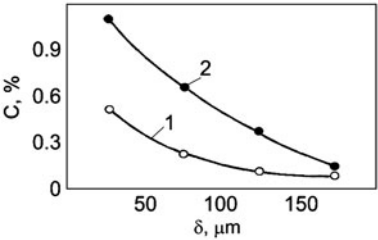


Fig. 2.7 Dependence of $\lg C$ on δ (1) and δ^2 (2) for saturation of the surface by carbon during MPT

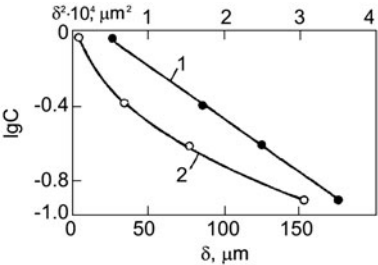
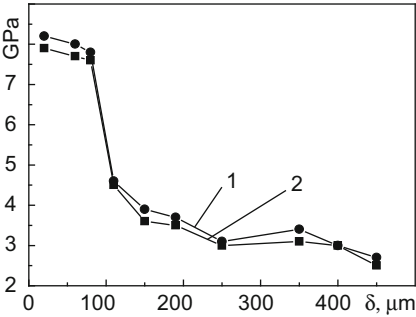


Table 2.1 Mass-spectral analysis of surface nanocrystalline layer, obtained by MPT on 40Kh steel in different coolants

Type of TE	Amount of elements on surface, in relative units			
	H ₂	N ₂	O ₂	C
Without MPT	1.0	1.0	1.0	1.0
MPT in mineral oil	3.0	1.7	1.2	2.3
MPT in aqueous environment	2.3	1.0	2.2	1.1

Fig. 2.8 Microhardness distribution of 45 steel in depth from surface after MPT in the special coolant for carburization (1) and mineral oil (2)



mechanical properties of steels. Useful additives while diffusing into grain boundaries increase the grain boundary energy, which results in increase of intergranular fracture energy. Therefore, the chemical composition of coolants affects the mechanical properties of surface NCS.

It is generally acknowledged that NCS in the bulk material improves its mechanical properties [15, 21, 22, 25, 26]. This was proved also for the surface NCS [7, 18]. It is shown in the example of strengthening by MPT (Fig. 2.8) that the surface

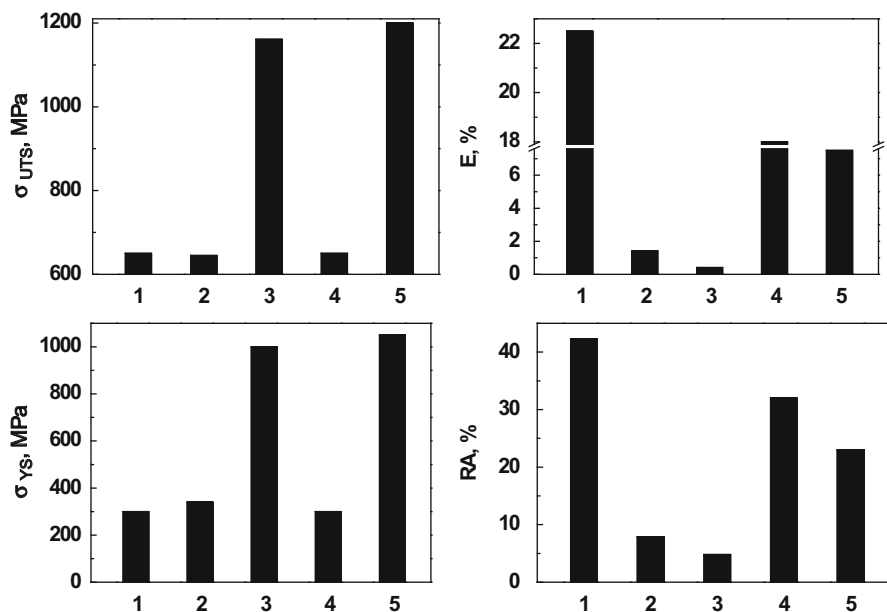


Fig. 2.9 A change of the mechanical properties of 65G steel specimens (Fig. 2.2) after MPT in the different coolants: 1—as-received state; 2, 3—MPT in aqueous TE; 4, 5—MPT in mineral oil; 2, 4—as received state + MPT; 3, 5—quenching + tempering at 500°C + MPT + tempering at 500°C

microhardness of the 45 steel reaches 8–8.5 GPa after the MPT, which is three times higher than for the original material.

Changes in the mechanical properties of the high-carbon 65G steel after MPT ($V_2 = 1.0$ m/min; $S = 0.5$ mm/double motion; $t = 0.3$ mm) are presented in Fig. 2.9. The tensile strength changed insignificantly and independent of the coolant type. However, the plastic

behaviour, the elongation in particular, varies with the coolant type. Such behaviour is caused due to carbon, oxygen and hydrogen, which are segregated mainly at grain boundaries and affect the grain boundary strength. The surfaces of flat specimens pretreated by MPT with different coolants and then subjected to tensile loading are presented in Fig. 2.10. Numerous microcracks can be observed in the case of aqueous coolant.

Wear-resistance tests of the 40Kh steel showed (Fig. 2.11) a positive effect of MPT in comparison with quenching and low tempering. The wear resistance was increased for both hardened rings and not-hardened inserts. It is caused by a substantial decrease of the friction.

The applied MPT also had a positive effect on the fatigue crack growth resistance of the 40Kh steel (Fig. 2.12). The fatigue test results show the lowest crack growth rate dA/dN for the specimens treated in mineral oil (curve 3) and the highest crack growth rate dA/dN for the untreated specimens (curve 1). This is in good agreement with the X-ray examinations showing a lower-surface grain size of 19 nm for the

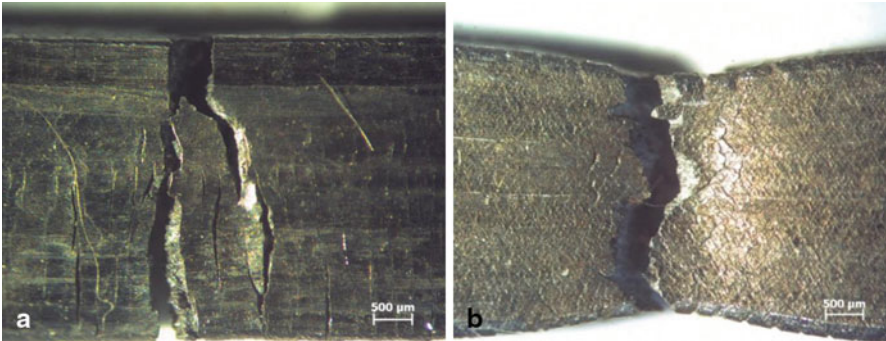


Fig. 2.10 Treated by MPT, the 65G steel specimens after the tension test: **a** in aqueous MPT and **b** mineral oil coefficient from 0.14–0.16 at quenched state to 0.04–0.06 after the MPT in mineral oil [11]. Such effects can be explained by a change of contribution of electrons of *d*-orbitals in metallic bonding [1].

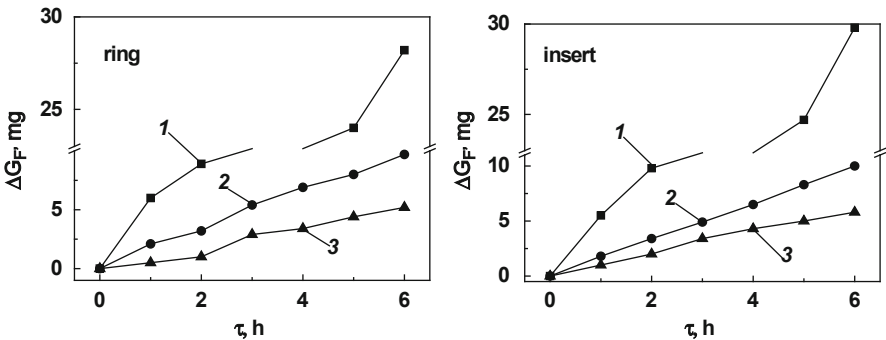


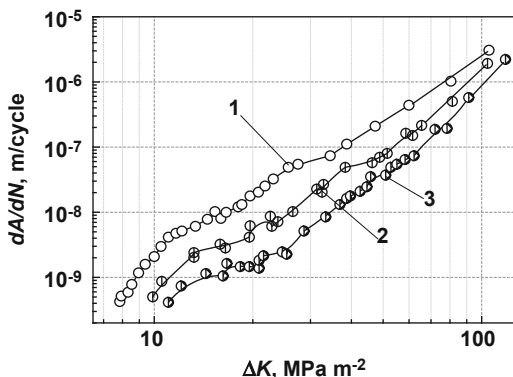
Fig. 2.11 Wear kinetic of the couple 40Kh–ShKh15 in the oil-abrasive environment (MPT regimes, $V_2 = 1.0$ m/min, $S = 0.5$ mm/double motion, $t = 0.3$ mm): 1—quenching and low tempering; 2—MPT in aqueous coolant; 3—MPT in mineral oil

specimen treated in mineral oil than for the specimen treated in the aqueous coolant (24 nm).

2.4 Conclusions

The surface gradient nanocrystalline structure is formed during MPT by severe thermal-plastic deformation. The phase transformations and the changes of the chemical composition of surface layers take place due to the very fast heating and cooling as well as due to alloying by the coolant additives. The mechanical properties of the hardened layers substantially depend on the coolant type, which affects the grain

Fig. 2.12 Fatigue crack growth rate dA/dN in 40Kh steel: 1—without MPT, 2—MPT in aqueous coolant, 3—MPT in mineral oil



boundary strength by segregation of carbon, oxygen and hydrogen. Such structures are characterized by improved mechanical properties: higher tensile strength and yield stress, higher microhardness, wear resistance and fatigue crack growth resistance.

References

1. Buckley DH (1981) Surface effects in adhesion, friction, wear, and lubrication. Elsevier, New York
2. Fisher JC (1951) Calculation of diffusion penetration curves for surface and grain boundary diffusion. J Appl Phys 22:74
3. Hunger H-J et al (1983) Ausgewelte Untersuchungsverfahren in der Metalkunde. VEB Deutscher Verlag für Grundstoffindustrie. Leipzig
4. Hull D, Bacon DJ (2011) Introduction to dislocations. Elsevier, New York
5. Krous W, Nolze G (1996) Powder cell—a program for the representation and manipulation of crystal structures and calculation of the resulting x-ray powder patterns. J Appl Cryst 29:301–303
6. Kalichak TN, Kyryliv VI, Fenchin S (1989) Mechanopulsed hardening of long components of the hydraulic cylinder rod type. Sov Mater Sci 25(1):96–99
7. Kocanda D, Hutsaylyuk V, Slezak T, Torzewski J, Nykyforchyn H, Kyryliv V (2012) Fatigue crack growth rates of S235 and S355 steels after friction stir processing. Mater Sci Forum 726:203–210
8. Kuzydlowski KJ (2006) Physical, chemical, and mechanical properties of nanostructured materials. Mater Sci 42(1):85–94
9. Kyryliv VI (1998) Surface alloying of steels in the process of mechanical pulse treatment. Mater Sci 34(3):416–419
10. Kyryliv VI (1999) Surface saturation of steel with carbon during mechanikel-pulse treatment. Mater Sci 35(6):853–858
11. Kyryliv VI (2012) Improvement of the wear resistance of medium-carbon steel by nanodispersion of surface layers. Mater Sci 48(1):119–123
12. Kyryliv VI, Koval' YuM (2001) Surface alloying of steels from special process media. Mater Sci 37(5):816–819
13. Liu G, Lu J, Lu K (2000) Surface nanocrystallization of 316 Lstainless steel induced by ultrasonic shot peening. Mater Sci Eng A 286:91–95

Nanocomposites, Nanophotonics, Nanobiotechnology,
and Applications

Selected Proceedings of the Second FP7 Conference
and International Summer School Nanotechnology:
From Fundamental Research to Innovations, August
25-September 1, 2013, Bukovel, Ukraine

Fesenko, O.; Yatsenko, L. (Eds.)

2015, XX, 403 p. 197 illus., 85 illus. in color., Hardcover

ISBN: 978-3-319-06610-3